Comparative benefits of drone imagery for nitrogen status determination in corn

K. Khun[2], P. Vigneault[1], N. Tremblay[1], M.Y. Bouroubi[4], F. Cavayas[2] and C. Codjia[3]

[1] *R&D Centre, Agriculture and Agri-Food Canada, Saint-Jean-sur-Richelieu, QC, Canada*

[2]*Department of Geography, University of Montreal, Montreal, QC, Canada*

[3]*Department of Geography, Université du Québec à Montréal, Montreal, QC, Canada*

[4]*Effigis GeoSolutions, Montreal, QC, Canada*

A paper from the Proceedings of the
13th International Conference on Precision Agriculture
July 31 – August 4, 2016
St. Louis, Missouri, USA

Abstract. *Remotely sensed vegetation data provide an effective means of measuring the spatial variability of nitrogen and therefore of managing applications by taking intrafield variations into account. Satellites, drones and sensors mounted on agricultural machinery are all technologies that can be used for this purpose. Although a drone (or unmanned aerial vehicle [UAV]) can produce very high-resolution images, the comparative advantages of this type of imagery have not been demonstrated. The goal of this study was to assess the potential benefits associated with the high spatial resolution (5 cm per pixel) of drone-acquired images in comparison to a proximal sensor used for nitrogen status determination in corn. A series of images were acquired over two commercial fields in June 2015. The corn phenological stages at the time of data acquisition ranged from V4 to V6. Images were acquired from a UAV (eBee fixed-wing drone) and from GreenSeeker onboard sensors. The UAV was operated with a modified commercial camera: the Canon S110 NIR (550 nm, 625 nm and 850 nm). Field measurement campaigns were carried out and coordinated with image acquisition in order to obtain quantitative measurements of the biophysical parameters governing vegetation conditions (biomass and leaf area index [LAI]). To assess the potential benefits of image segmentation, a comparative analysis of normalized difference vegetation index (NDVI) maps produced from the GreenSeeker and UAV data was carried out. NDVI maps generated from UAV imagery contained higher spatial detail than those produced by GreenSeeker, but both technologies had good relationships with biomass and LAI. The GreenSeeker R^2 relationships with biophysical parameters outperformed those of the UAV.*

Keywords. *Unmanned aerial vehicle, UAV, GreenSeeker, eBee, spatial resolution, nitrogen, leaf area index, biomass, NDVI, image processing, image classification.*

Introduction

Remote N status assessment in corn is normally carried out by using a vegetation index or by estimating biophysical parameters such as biomass, leaf area index (LAI) and chlorophyll. The recent introduction of drones or unmanned aerial vehicle (UAV) platforms offers yet another option for remote N status assessment in corn. They can be deployed quickly and have very high spatial resolution.

Zhang and Kovacs (2012) produced a detailed review of the uses, potential and limitations of UAVs for precision agriculture. Hunt et al. (2013) summarized the problems and opportunities of using UAV sensing for quantitative measurements in crop assessment. They suggested that the approach of downscaling by averaging pixel values did not take advantage of the existence of pure endmembers of leaves, soil and shadow in images with such a high spatial resolution. A very high spatial resolution offers the opportunity to apply segmentation procedures that separate spectral information for vegetation from background information, as shown in Torres-Sánchez et al. (2014). Compared with onboard sensors such as the GreenSeeker, UAV imagery makes it possible to focus on crop-based information by excluding spectral information for soil or weeds.

Tremblay et al. (2014) compared UAV imagery (25-cm resolution) and Pléiades-1B satellite imagery (2-m resolution) acquired within 4 d of each other over a corn crop at early stages suitable for in-season nitrogen application. The soil-adjusted vegetation index (SAVI; Huete 1988) acquired from the UAV was better correlated with fresh biomass than that from the satellite (R^2 = 0.93 for the UAV vs. R^2 = 0.88 for the satellite). However, image segmentation on the UAV imagery improved R^2 with fresh biomass by only 0.03 points. It tended to narrow the dynamic range of the SAVI. Rey et al. (2013) reported that the correlation of multispectral UAV imagery with vine vigor and yield parameters required very complex processing in order to be useful for quantitative measurement of biophysical parameters. Tremblay et al. (2014) also found that additional care was needed to make radiometric corrections (vignetting reduction and bidirectional reflectance distribution function [BRDF] influences) to UAV images. While comparisons of UAV with satellite imagery exist, no examples of comparisons with onboard sensors were found in the literature. The objective of this study was therefore to compare fixed-wing UAV imagery to GreenSeeker onboard sensor measurements in the context of remote N status assessment.

Materials and methods

Field site

The experiment was conducted in the summer of 2015 on corn (*Zea mays* L.) at growth stages V4 to V6 in two commercial fields. The fields, designated as Field 1 (45°16′35.78″ N, 73°17′26.48″ W) and Field 2 (45°14′23.22″ N, 73°23′53.72″ W), were located near Saint-Jean-sur-Richelieu in southern Quebec, Canada. Field 1 was relatively small (2.9 ha) and flat and contained areas infested primarily by yellow nut sedge (*Cyperus esculentus* L.). Field 2 was larger (12.9 ha), had a small rise in the midfield area and ended with a slight topographic depression. Field 2 contained areas where field horsetail (*Equisetum arvense* L.) was significantly present.

GreenSeeker Acquisition and Processing

The GreenSeeker Variable Rate Application and Mapping Systems (Trimble, Sunnyvale, CA) is a commercially available sensor capable of measuring canopy reflectance. It is an active system that produces its own light source: two light-emitting diodes (LEDs) illuminate the ground at two specific wavelengths, namely 656 nm (RED) and 774 nm (near infrared [NIR]). The normalized difference vegetation index (NDVI) is by far the best known vegetation index (Steven et al. 2015) and can be

calculated by combining those two spectral bands:

NDVI = (NIR − RED) / (NIR + RED)

The NDVI was originally derived from satellite imagery (Rouse et al. 1974) but is now being obtained with active sensors, such as the GreenSeeker, and used as a proxy for plant biophysical properties and for remote N status assessment (Hatfield et al. 2008; Samborski et al. 2009; Shaver et al. 2009).

In our experiment, a GreenSeeker unit with eight heads was used to measure vegetation vigor, expressed as the NDVI. The tractor-mounted GreenSeeker was operated on June 12 in Field 1 and on June 18 in Field 2. The swath width of each GreenSeeker head was approximately 60 cm. The sensor heads were oriented and positioned directly over eight rows. The onboard computer was connected directly to the tractor's automated steering system, equipped with a real-time kinematic (RTK)-enhanced GPS (Trimble, Sunnyvale, CA). The tractor speed was approximately 7.2 km h^{-1} in order to achieve 2-m spacing between each data recording.

Each GreenSeeker point measurement was in fact the mean NDVI value as measured by the eight heads over the area scanned by the sensor since the last acquisition point. Its real footprint was therefore a rectangle whose dimensions corresponded to the swath width of the eight heads (i.e. 6 m) and the distance travelled by the tractor between two GPS points (i.e. about 2 m, depending on the tractor speed). For each GreenSeeker record, the corresponding footprint was digitized in ArcGIS (ESRI, Redland, CA) and assigned the measured NDVI value ($NDVI\_GS_{6\times2m}$), as shown in Figure 1. $NDVI\_GS_{6\times2m}$ was used for comparison with the UAV-derived NDVI.

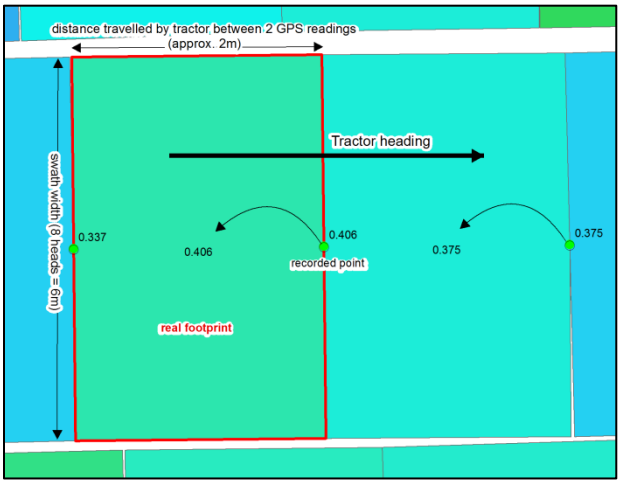

Figure 1. GreenSeeker-recorded value translated into its real footprint ($NDVI\_GS_{6\times2m}$), used for comparison with UAV data.

A Python script was used to extract the location, as well as the value of each head recording. This made it possible to obtain the crop vigor for each row, rather than an average value over eight rows. The point dataset was then interpolated through kriging with the GS+ software (Gamma Design, Plainwell, MI). The grid size of the interpolated raster ($NDVI\_GS_{1m}$) was set to 1 m for mapping and data analysis (Figure 2). $NDVI\_GS_{1m}$ was used for comparison with ground-truth points.

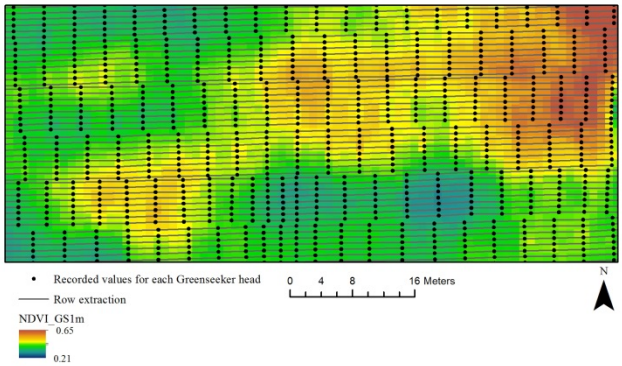

Figure 2. NDVI_GS$_{1m}$ map after kriging, used for comparison with ground-truth data. Aligned points represent the GreenSeeker-recorded values during the tractor movement.

UAV Image Acquisition and Processing

A converted commercial 12-megapixel camera (Canon Powershot S110) was used to acquire images at a very high spatial resolution (<5 cm). After conversion, the blue channel became NIR (850 nm), while the green (550 nm) and red (625 nm) channels remained the same. The camera was mounted on a fixed-wing UAV (eBee Ag unit, senseFly SA, Cheseaux-Lausanne, Switzerland), which was owned and operated by the Department of Geography of the Université du Québec à Montréal (UQAM; Montreal, Quebec, Canada). The campaign was carried out on June 13, 2015, for Field 1 and on June 17, 2015, for Field 2 in the middle of the day (between 10 AM and 2 PM) under a clear sky with winds less than 15 km h^{-1}, at mean altitudes of 150 m (Field 1) and 140 m (Field 2). Flight planning and monitoring was performed by the built-in software eMotion 2 (senseFly SA, Cheseaux-Lausanne, Switzerland).

In order to increase image stitching success, a minimum overlap of 70% (side-lap and forward-lap) was planned for each flight path. The raw images were converted to TIFF files and then imported into Pix4Dmapper Pro software (Pix4D, Lausanne, Switzerland). A georectified orthomosaic was generated using ground control points (GCPs) located in the fields and positioned with an RTK-based GPS receiver (SXBlue III-L, Geneq Inc., Montreal, Quebec, Canada).

An image of a Spectralon panel (Labsphere Inc., North Sutton, NH) was taken before each flight and used by Pix4Dmapper Pro to calibrate the spectral data. Further radiometric processing was performed by the software to correct the rolling shutter effect, and pixel values were averaged from overlapping images to reduce the BRDF. A reflectance map with a resolution of 5 cm could then be produced and used to calculate the NDVI (NDVI_UAV$_{5cm}$).

The UAV-based NDVI map was then segmented into two classes—vegetation and bare soil—using Otsu's thresholding method (Otsu 1979). This algorithm automatically calculates the optimum threshold in a gray-level image that maximizes the inter-class variance.

In order to compare the performances of the UAV and GreenSeeker performances, each GreenSeeker footprint was assigned the mean value of the contained pixels from the NDVI_UAV$_{5cm}$ map, generating a resampled map (NDVI_UAV$_{6x2m}$). It was then possible to analyze NDVI_GS$_{6x2m}$ and NDVI_UAV$_{6x2m}$.

Ground-truthing

A ground-truthing campaign was conducted to collect biomass and LAI data. These points were compared with data extracted from UAV and GreenSeeker images given that only less than 3 days separated the UAV flights and GreenSeeker acquisition and the ground-truth campaign.

A stratified sampling strategy based on two-layer spatial constraints (NDVI_GS$_{1m}$ map and N treatment strips) was used, that identified a pool of 30 and 40 points respectively for Fields 1 and 2. Each point was positioned with an RTK-based GPS receiver (SXBlue-III L; Geneq Inc., Montreal,

QC, Canada) that was accurate to 5 cm. An area covering two rows by one linear meter was defined from each sampling point. The real location of the sampled areas was shifted sideways to cover the two nearest rows and, if needed, along the rows to avoid abnormally scarce vegetation. Corresponding LAI measurements were taken with an LAI-2200 instrument (Li-Cor Inc., Lincoln, NE). Fresh biomass was sampled, weighed, dried, weighed again and used to correlate with the remote sensing parameters.

In order to analyze the collected data, all the sampling points were superimposed on the cell grids derived from the GreenSeeker map and the UAV imagery. Each sampling point was associated with the pixel on the $NDVI\_GS_{1m}$ map located at exactly the same coordinates. As for the UAV imagery, a 1.5 × 1 m rectangle (the "*in situ* plot") corresponding to each sampled area was created and assigned the mean value of the pixels within that polygon ($NDVI\_UAV_{plots}$). To further capitalize on the high spatial resolution offered by the UAV images, the crop rows within each sampled area (the "*in situ* rows") were manually delineated, and the pixels included in those rows alone were averaged to obtain a second NDVI mean value ($NDVI\_UAV_{rows}$). At the same time, the vegetation pixels classified as corn (i.e. vegetation located in the delineated rows) were counted. The ratio of the number of corn pixels to the total number of pixels in each plot could then be calculated to assess the vegetation cover fraction (VCF).

Results and Discussion

Comparison of NDVI Maps

Figure 3a and Figure 3b illustrate how both sensors (UAV onboard camera and tractor-mounted GreenSeeker) perceive the NDVI variations in Field 1. As expected, the $NDVI\_GS_{1m}$ map showed less detail than the $NDVI\_UAV_{5cm}$ map. The patterns highlighted by both maps were very similar, but crop rows were perfectly visible in the UAV-based map (Figure 3b, inset b1). Areas infested by weeds (higher NDVI in red, Figure 3b, inset b2) could be seen clearly, whereas they could only be guessed from the GreenSeeker map (Figure 3a, inset a2).

The NDVI value range was wider for the UAV-based map, due to its pixel heterogeneity (Figure 3b), which ranged from −0.10 to 0.85: at a resolution of 5 cm, most pixels were pure endmembers representing either crop, weed, soil or shadow. In the GreenSeeker map (Figure 3a), the NDVI values ranged from 0.21 to 0.65: since each scanned area was spectrally mixed, the NDVI calculated from the mean reflectances had a narrower range of values. Similar results were observed in Field 2 (data not shown).

The NDVI assigned to each GreenSeeker footprint was used to further compare the sensors ($NDVI\_GS_{6\times2m}$ and $NDVI\_UAV_{6\times2m}$). A linear regression was performed with both datasets, resulting in high correlations (Figure 4). However, the $NDVI\_UAV_{6\times2m}$ values were greater than $NDVI\_GS_{6\times2m}$ at the low end but similar at the high end of the NDVI range. Field NDVI distributions are therefore sensor dependent (just as in Tremblay et al. 2008), a finding that has agronomic implications for crop management, such as variable N rate recommendations.

Based on these high correlations, $NDVI\_GS_{6\times2m}$ was used to predict $NDVI\_UAV_{6\times2m}$. A difference map was produced on a standard deviation basis, comparing the predicted $NDVI\_UAV_{6\times2m}$ and measured $NDVI\_UAV_{6\times2m}$ values for Field 1 (Figure 3c). The areas where the measured $NDVI\_UAV_{6\times2m}$ value was higher than its predicted value perfectly matched the areas infested by weeds. Similar results were observed in Field 2 (data not shown).

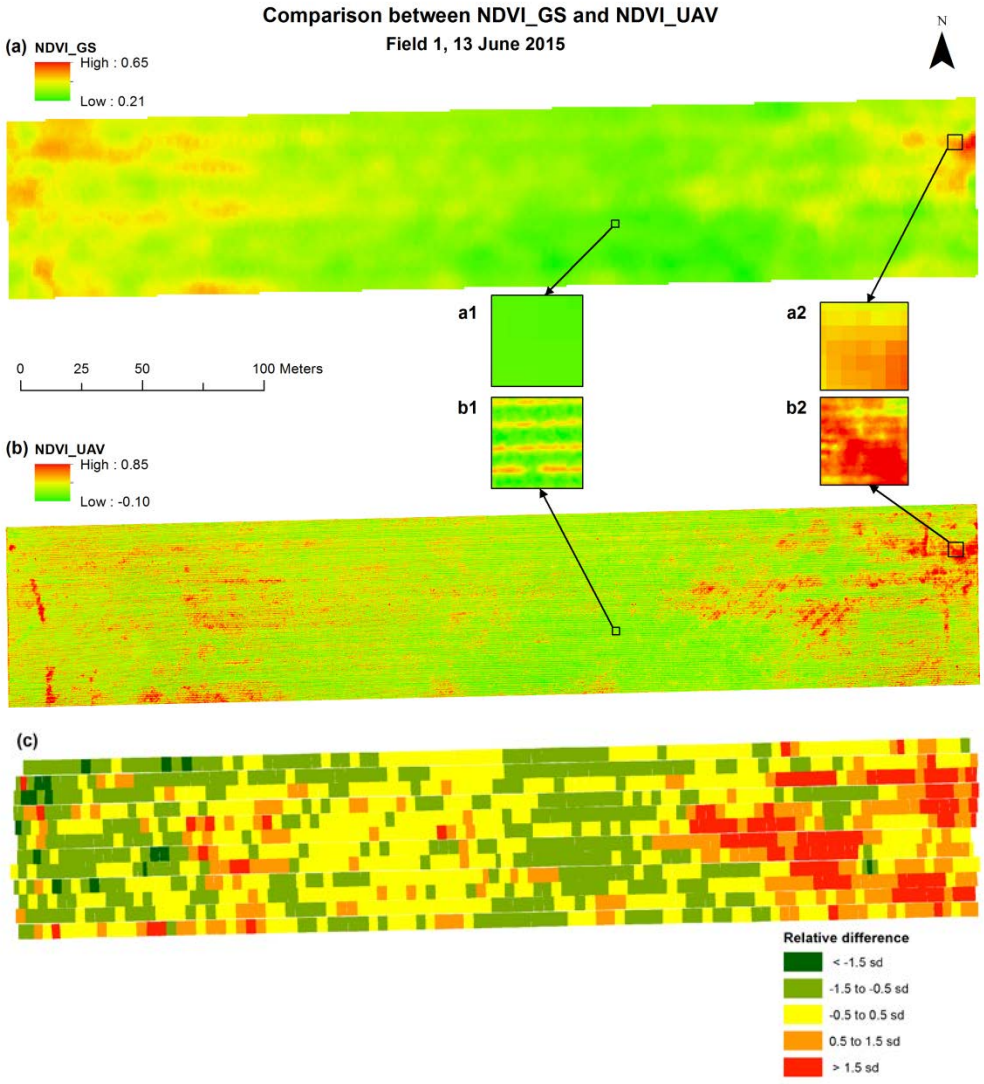

Figure 3. Comparison between a) NDVI_GS$_{1m}$ and b) NDVI_UAV$_{5cm}$ maps. After a linear regression, c) a residual map shows the relative difference between the measured and predicted NDVI_UAV$_{6\times2m}$ for each GreenSeeker footprint (sd: standard deviation).

That result could be explained in part by the different viewing geometries of the two sensors. Since the GreenSeeker heads were positioned directly over the corn rows and their swath width was only 60 cm (smaller than the 75-cm inter-row spacing), NDVI_GS$_{6\times2m}$ was more sensitive to the corn canopy and less sensitive to the weeds and soil located further below in the inter-rows. In contrast, NDVI_UAV$_{6\times2m}$ was averaged from all pixels (including those in the inter-rows) located within the GreenSeeker footprint. Since the UAV image pixels after orthorectification were viewed from the nadir, every pixel within the 6 × 2 m footprint had an equal weight in the calculation of the mean NDVI. Therefore, the presence of weeds contributed more to the NDVI_UAV$_{6\times2m}$ than to the NDVI_GS$_{6\times2m}$.

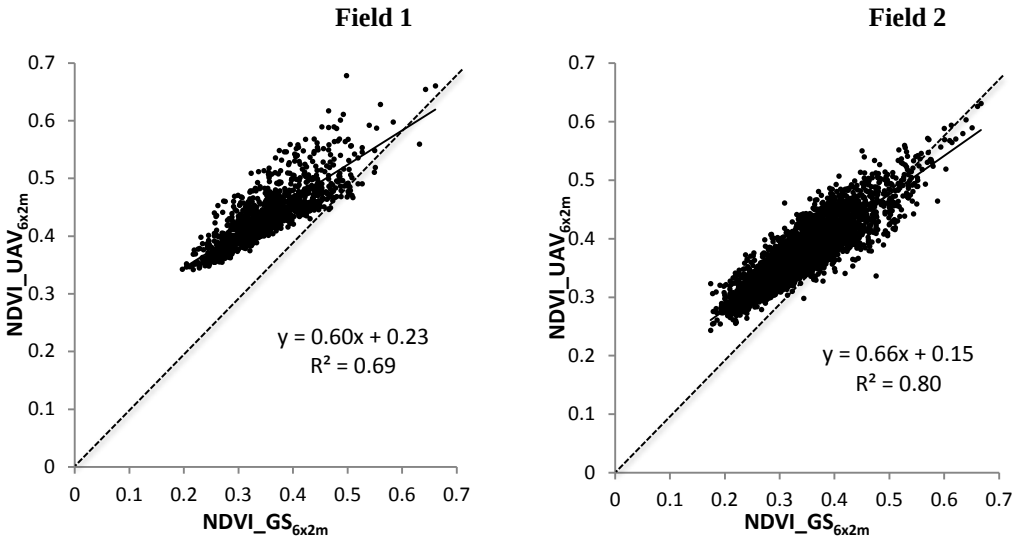

Figure 4. Relationships between $NDVI\_GS_{6\times2m}$ and $NDVI\_UAV_{6\times2m}$ for fields 1 and 2.

Comparison Between NDVI (UAV and GS) and Ground-Truth Points

There was a linear relationship between sampled biomass and $NDVI\_UAV_{plots}$ for Field 1 (R^2 = 0.33) and Field 2 (R^2 = 0.34). When only the pixels inside the two crop rows for each sampling area ("*in situ* rows") were considered, the relationship between $NDVI\_UAV_{rows}$ and biomass was slightly higher: R^2 = 0.34 (Figure 5a) and R^2 = 0.39 (Figure 5b) respectively for fields 1 and 2. The R^2 between LAI and $NDVI\_UAV_{rows}$ was 0.33 for both fields. Lelong et al. (2008) observed a similar linear relationship between LAI and NDVI_UAV in experiments conducted on wheat at early stages. Hunt et al. (2014) found a correlation coefficient of 0.58 when they compared the Green NDVI and biomass at the plot scale. These studies used replicated microplots, whereas the present study was conducted on large-scale commercial fields with orthomosaicked images.

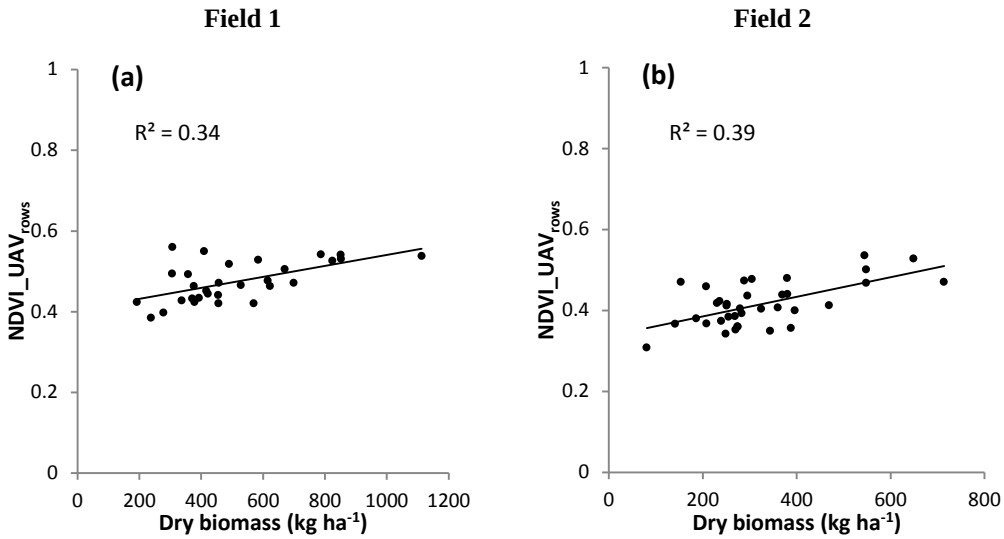

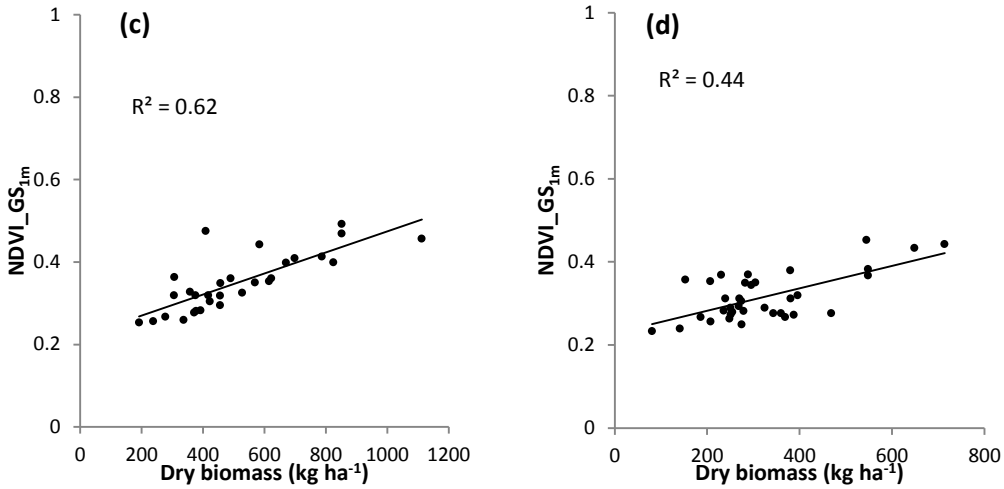

Figure 5. Relationship between dry corn biomass and NDVI (UAV and GS) for fields 1 (a, c) and 2 (b, d). NDVI_UAV$_{rows}$ was calculated for *in situ* rows.

From Figure 5, it can be concluded that NDVI_GS data outperformed NDVI_UAV. Indeed, the R^2 between NDVI_GS$_{1m}$ and dry biomass was higher than NDVI_UAV$_{rows}$ for both fields. Hong et al. (2007) also found that NDVI measured by the GreenSeeker resulted in a good correlation with corn dry weight at stage V6 to V7 (r = 0.79).

Several factors could explain the better results produced by the GreenSeeker, including the following:

1) The geographic positioning accuracy of the *in situ* plots. Their GPS coordinates, though provided by the RTK system, were not completely accurate. These coordinates were the theoretical ones generated randomly beforehand. Once in the fields, however, the real location of each sampled area was slightly shifted. NDVI_GS$_{1m}$ was extracted from a kriged map, which was more robust for outlying values and spatial inaccuracies in plot positioning. Indeed, kriging tended to smooth the NDVI values for neighboring areas. Outliers had less impact, and plot positioning could tolerate an imprecision of a few meters. In contrast, mean NDVI_UAV$_{plots}$ values could be markedly different if the plot was erroneously shifted a few centimeters along the two rows, or worse, over different rows. Furthermore, the slight georeferencing errors in UAV images may have increased that spatial inaccuracy.

2) The radiometric accuracy of UAV images. Owing to its mode of acquisition, the UAV imagery contained noises inherent to lighting conditions (shadows, specular reflections, hot spot effects, canopy BRDF), sensor defects (vignetting, roller shutter, full-spectrum, etc.), and viewing geometry due to the unstable behavior (roll, pitch, yaw) of fixed-wing aircraft. Those effects were reported by Zhang and Kovacs (2012) in their review of UAV applications in precision agriculture. BRDF effects were expected to play an important role in reflectance correction, but little research has been done into their impact on UAV high-resolution imagery (Rasmussen et al. 2016). Orthomosaicking also decreased image quality through resampling, which generated a blurry image, where pure pixels became spectrally mixed. As an active sensor, the GreenSeeker was less influenced by lighting conditions and image preprocessing.

Link et al. (2013) recommended a high density of images to improve data quality. This was achieved for Field 1 in this study, where the flight path was supplemented with a perpendicular flight. Field 2 was too large, and a flight path of this kind would have required excessive operational time, combined with multiple UAV landings and takeoffs to replace batteries, which would ultimately have resulted in varying lighting conditions during data acquisition. The image stitching for Field 2 therefore contained some defects, and those areas were removed from data analysis.

Since UAV imagery offered a very high resolution, pixel counting (VCF) was used as a method of assessing crop vigor, as was done by Rasmussen et al. (2013) and Torres-Sánchez et al. (2014). However, using VCF did not improve the correlation with dry biomass. In fact, R^2 was reduced to 0.18 and 0.15 respectively for fields 1 and 2 (data not shown). Here again, the same factors (plot location and image quality) affected the results, the more so because the pixel-counting technique requires very high-quality data. A finer spatial resolution would have been necessary. Rasmussen et al. (2013) found that crop/soil segmentation at early growth stages in barley required ultrafine-resolution images (<5 mm per pixel). Hunt (2014) used simulated UAV images with a resolution of 1 mm. In order to maintain image sharpness, a multicopter was used instead of a fixed-wing UAV, and orthomosaicking was not applied in those experiments.

Table 1. Summary of the GreenSeeker and UAV sensing limitations outlined in this paper.

	GreenSeeker sensing	UAV sensing
Spatial information	Low resolution but focused on the crop row with little influence from the inter-rows	High resolution, depending on the camera resolution and the UAV altitude and speed
Spectral information	Few spectral bands, usually two (visible and NIR)	Options for RGB, multispectral or thermal cameras
Radiometric information	Slightly influenced by lighting conditions (Barker et al. 2013) Dependent on tractor speed (Shaver et al. 2010)	Dependent on lighting conditions and sensor opto-geometric parameters: Vignetting (Lelong et al. 2008) BRDF (Lelong et al. 2008) Atmospheric noise (Berni et al. 2009) and adjacency effects Quality reduced by resampling due to geometric preprocessing (fixed-wing UAV): Orthorectification Mosaicking

Conclusion

UAV imagery is currently the focus of much interest, including for driving variable nitrogen rate applications. This study compared UAV imagery with an industry standard for that purpose in a field operation context that included the presence of weed patches. Owing to its mode of operation, the GreenSeeker produced an NDVI map with a lower spatial resolution than that of UAV imagery. However, because the GreenSeeker is an active system, its radiometric information was less influenced by lighting conditions. Contrary to our initial hypothesis, the GreenSeeker map was not significantly affected by soil or weed effects compared with UAV imagery. Although highly correlated, the NDVI maps did not exhibit the same frequency distributions, which means that any use for site-specific management should take the difference into account. Pixel counting of VCF did not produce results that would improve the relevance of UAV imagery, whose low radiometric quality and limited spatial resolution (5 cm) prevented a precise delineation of corn leaves. Further experiments need to be conducted with higher-resolution images (<1 cm) acquired from a multicopter UAV in order to determine to what extent the observed inaccuracies resulted from the limitations inherent to a fixed-wing UAV setup.

Acknowledgements

The authors would like to acknowledge the fine contributions of Edith Fallon, Carl Bélec, Marcel Tétreault, Mohamed Yacine Bouroubi, Julie Surprenant, and the farmers Claude Lanciault and Jérôme Letellier.

References

Barker, D. W., & Sawyer, J. E. (2013). Factors affecting active canopy sensor performance and reflectance measurements. *Soil Science Society of America Journal*, 77(5), 1673–1683.

Berni, J. A. J., Zarco-Tejada, P. J., Suárez, L., & Fereres, E. (2009). Thermal and narrowband multispectral remote sensing for vegetation monitoring from an unmanned aerial vehicle. *IEEE Transactions on Geoscience and Remote Sensing*, 47(3), 722–738.

Hatfield, J. L., Gitelson, A. A., Schepers, J. S., & Walthall, C. L. (2008). Application of spectral remote sensing for agronomic decisions. *Agronomy Journal*, 100(3 SUPPL.), S-117–S-131.

Hong, S.D., J.S. Schepers, D.D. Francis & M.R. Schlemmer. (2007). Comparison of ground-based remote sensors for evaluation of corn biomass affected by nitrogen stress. *Communications in Soil Science and Plant Analysis* 38(15-16), 2209-2226.

Huete, A. R. (1988). A soil-adjusted vegetation index (SAVI). *Remote Sensing of Environment*, 25(3), 295–309.

Hunt, E. R., Jr., Daughtry, C. S. T., Mirsky, S. B., & Hively, W. D. (2013). Remote sensing with unmanned aircraft systems for precision agriculture applications. In Proceedings of the Second International Conference on Agro-Geoinformatics: Information for Sustainable Agriculture. Fairfax, VA: Center for Spatial Information Science and Systems.

Hunt, E. R., Jr., Daughtry, C. S. T., Mirsky, S.B., & Hively, W.D. (2014). Remote sensing with simulated unmanned aircraft imagery for precision agriculture applications. *IEEE Journal of Selected Topics in Applied Earth Observations and Remote Sensing*, 7(11), 4566–4571.

Lelong, C. C. D., Burger, P., Jubelin, G., Roux, B. Labbé, S., & Baret, F. (2008). Assessment of unmanned aerial vehicles imagery for quantitative monitoring of wheat crop in small plots. *Sensors*, 8(5), 3557–3585.

Link, J., D. Senner & W. Claupein. (2013). Developing and evaluating an aerial sensor platform (ASP) to collect multispectral data for deriving management decisions in precision farming. *Computers and Electronics in Agriculture* 94, 20-28.

Otsu, N. (1979). A Threshold Selection Method from Gray-Level Histograms. *IEEE Transactions on Systems, Man and Cybernetics*, 9(1), 62–66.

Rasmussen, J., J. Nielsen, F. Garcia-Ruiz, S. Christensen & J.C. Streibig. (2013). Potential uses of small unmanned aircraft systems (UAS) in weed research. *Weed Research*, 53, 242-248.

Rasmussen, J., Ntakos, G., Nielsen, J., Svensgaard, J., Poulsen, R.N., & Christensen, S. (2016). Are vegetation indices derived from consumer-grade cameras mounted on UAVs sufficiently reliable for assessing experimental plots? *European Journal of Agronomy*, 74, 75–92.

Rey, C., Martín, M. P., Lobo, A., Luna, I., Diago, M. P., Millan, B., & Tardáguila, J. (2013). Multispectral imagery acquired from a UAV to assess the spatial variability of a Tempranillo vineyard. In J. V. Stafford (Ed.), Precision Agriculture 2013, Proceedings of the 9th European Conference on Precision Agriculture (pp. 617–624). Wageningen: Wageningen Academic Publishers.

Rouse, J. W., Haas, R. H., Schell, J. A., & Deering, D. W. (1974). Monitoring vegetation systems in the Great Plains with ERTS. In S. C. Freden, E. P. Mercanti, & M. A. Becker (Eds.), Proceedings of the Third Earth Resources Technology Satellite-1 Symposium (pp. 309–317). Washington, D.C.: NASA.

Samborski, S. M., Tremblay, N., & Fallon, E. (2009). Strategies to make use of plant sensors-based diagnostic information for nitrogen recommendations. *Agronomy Journal*, 101(4), 800–816.

Shaver, T. M., Khosla, R., & Westfall, D. G. (2009). Red and amber normalized difference vegetation index (NDVI) ground-based active remote sensors for nitrogen management in irrigated corn. In Proceedings of the 2009 Fluid Forum. Scottsdale, AZ: Fluid Fertilizer Foundation.

Shaver, T. M., Khosla, R., & Westfall, D. G. (2010). Evaluation of two ground-based active crop canopy sensors in maize: growth stage, row spacing, and sensor movement speed. *Soil Science Society of America Journal*, 74(6), 2101–2108.

Steven, M. D., Malthus, T. J., & Baret, F. (2015). Toward standardization of vegetation indices. In P. S. Thenkabail (Ed.), *Remotely Sensed Data Characterization, Classification, and Accuracies, Vol. 1* (pp. 175–194). New York: CRC Press.

Torres-Sánchez, J., Peña, J. M., de Castro, A. I., & López-Granados, F. (2014). Multi-temporal mapping of the vegetation fraction in early-season wheat fields using images from UAV. *Computers and Electronics in Agriculture*, 103, 104–113.

Tremblay, N., Wang, Z., Ma, B.-L., Belec, C., & Vigneault, P. (2008). A comparison of crop data measured by two commercial sensors for variable-rate nitrogen application. *Precision Agriculture*, 10(2), 145–161.

Tremblay, N., Vigneault, P., Bélec, C., Fallon, E., & Bouroubi, M. Y. (2014). A comparison of performance between UAV and satellite imagery for N status assessment in corn. In Proceedings of the 12th International Conference on Precision Agriculture (Paper 1681). Sacramento, CA: International Society of Precision Agriculture.

Zhang, C., & Kovacs, J. (2012). The application of small unmanned aerial systems for precision agriculture: a review. *Precision Agriculture*, 13, 693–712.